03

Influence of the near-surface plasma area on a supersonic flow past a semi-cylinder in different gases

© T.A. Lapushkina,[1] O.A. Azarova,[2] E.V. Reshetova,[2] K.I. Belov[1]

[1] Ioffe Institute,
194021 St. Petersburg, Russia
[2] Dorodnitsyn Computing Center, Federal Research Center „Computer Science and Control" Russian Academy of Sciences,
119333 Moscow, Russia
e-mail: tlapushkina@gmail.com

Received February 10, 2025
Revised April 14, 2025
Accepted May 11, 2025

The main objective of this study is to demonstrate the feasibility of actively influencing the position of the bow shock wave in a supersonic flow, as well as the parameters of an aerodynamic body, using a gas discharge generated near the frontal surface between the body and the bow shock wave. The dependence of the steady bow shock wave stand-off distance on the discharge power and current in xenon and air was studied experimentally and numerically. A comparison of the numerical and experimental data showed good agreement. It was found that the position of the steady bow shock wave is determined by the specific discharge power and the adiabatic index (affected by the degree of ionization and the degree of nonequilibrium) in the plasma zone created by the discharge. It was found that, at the initial stage, the dependence of the relative stand-off on the discharge power is close to linear, while the adiabatic index is close to constant. As the discharge current and power increase, the adiabatic index tends to increase in xenon and decrease in air. At the same time, an oscillatory dependence of the position of the steady bow shock wave on the discharge power was observed in xenon. This oscillation is associated with the possibility of the adiabatic index either increasing or decreasing depending on the correlation of plasma characteristics. Thus, it was shown that the adiabatic index of a gas-discharge plasma plays a significant role in the dynamics of the flow structure and the magnitude of the stand-off position of the steady bow shock wave from the body. The obtained results can be used in developing high-speed flow control systems, taking into account not only thermal effects but also the influence of plasma parameters.

Keywords: flow control, xenon, air, gas discharge, adiabatic index, bow shock wave, supersonic flow.

DOI: 10.61011/TP.2025.12.62406.20-25

Introduction

The task of controlling the bow shock wave (BSW) in front of the body is an important aspect of research on high-speed flow control, since the distance to the BSW directly affects the aerodynamic characteristics of the streamlined body. Research reviews on the use of energy investment for flow/flight control have been published [1–3]. The formation of complex spatial plasma structures and their effect on high-speed flow is described in review in Ref. [4]. An overview of studies of the interaction of air flow with various surface gas discharges is presented in Ref. [5], and experiments on controlling supersonic flow structures using surface discharges are discussed.

The theoretical aspects of the effect of energy release in the flow on the shock wave in front of the body and the parameters of the aerodynamic body were discussed in Ref. [6,7]. Experimental studies have shown the possibility of a significant effect on supersonic flow using various methods, including exposure to microwave energy (see Ref. [4]), laser pulses [8], electrical discharges [9], magneto-hydrodynamic effects [10].

The effect of an arc gas discharge on the position of an inclined shock wave was investigated in Ref. [11] and explained by thermal effects. In Ref. [12] the authors studied the possibility of controlling a cylindrical shock wave in front of a body and changing the angle of inclination of the wave when exposed to surface arc plasma. These phenomena were explained by the heating of the gas, which causes the deformation of the shock wave in front of the body.

It should be noted that among the studies on the control of BSW by energy supply to the flow, the effect of the degree of ionization and the degree of non-equilibrium has been relatively poorly studied. However, the introduction of charged particles, such as electrons and ions, into the gas flow near the aerodynamic body, together with thermodynamic non-equilibrium, characterized by an excess of the electron temperature over the gas temperature, leads to an additional displacement of the BSW compared to a purely thermal effect. Experimental data from studies of thermodynamically nonequilibrium flows near an aerodynamic body were compared in Ref. [13] with simulation results suggesting a thermal mechanism of discharge action. Experiments have shown that the effect of plasma on the dynamics of the shock wave is associated with nonequilibrium ionization in the flow. The dependence of the adiabatic index and specific heat capacities on the

degree of ionization and the degree of non-equilibrium for monatomic and diatomic plasmas was obtained in Ref. [14].

The effect of a gas discharge near the surface of a streamlined body on the position of the BSW in front of the body is studied in Ref. [15]. The study included the use of electrodynamic methods to influence the position of the BSW. Experimental results for a Mach 2 flow have shown that an increase in the power of a gas discharge near the surface of a body leads to an increase in the distance to the shock wave. Numerical calculations have shown that this shift is related to both thermal effects and plasma characteristics such as thermodynamic non-equilibrium and ionization. The control of supersonic air flow at Mach 4 near an aerodynamic body using energy input on the surface is described in Ref. [16]. It is shown that the deposition of energy in the near-surface area of the flow makes it possible to influence the position of the stationary BSW in front of the body and the aerodynamic characteristics of the body. These conclusions were confirmed by studies of the effect on the high-speed flow in the near-surface plasma region in xenon [17].

This study continues the studies of the possibility of controlling shock wave configurations by non-mechanical methods in Ref. [16,17]. The possibility of controlling the parameters of supersonic flow past a body by contributing energy to the region between the stationary BSW and the body, namely, by creating a gas-discharge plasma zone near the surface of the leading edge of the body, is studied. The purpose of this paper is to show the possibility of a local impact on the position of the BSW and the aerodynamic drag of a body by plasma action in the near-surface region and to compare the efficiency of this impact when gases flow around with different adiabatic indices, namely supersonic xenon flow and airflow. The results obtained can be useful for the development of new energy methods for controlling high-speed flow/flight based not only on thermal effects, but also on the influence of plasma parameters in local regions formed in the flow.

1. Experimental results

1.1. Setting up the experiment

The experiments were conducted using a setup based on an shock tube. A diagram of the gas dynamic path is shown in Fig. 1, *a*. The low pressure chamber *1* is connected to the working chamber *2*, which has a flat reflecting wedge-shaped supersonic nozzle with a wall angle of 11° relative to the axis and a width of 36 mm. The working chamber is separated from the low-pressure chamber by a thin lavsan diaphragm. The shock-compressed working gas is braked at the end of the low-pressure chamber, ionizes, and after the separation diaphragm is ruptured, it enters the nozzle through an inlet slit with a height of 5 mm with stagnation parameters, where the supersonic flow accelerates. The working chamber is connected to a damping tank *3*, where the exhaust gas is discharged. The installation additionally includes a gas discharge generation system based on LC circuits designed to organize rectangular current pulses of varying intensity and duration up to 600 μs.

A blunted semi-cylindrical model *4* with a diameter of the rounded part of $D = 3 \cdot 10^{-2}$ m and a length of 3.8 cm is located on its axis at a distance of 23 cm from the nozzle inlet. The model is clamped between two viewing side windows, the width of the model corresponds to the width of the channel 36 mm. In the model, copper electrodes with a width of 5 mm and a length of 30 mm are mounted above and below in the transition area of the cylindrical part to the horizontal, as shown in Fig. 1, *b*. The electrodes are connected to an external voltage source that generates a gas-discharge current near the front blunted edge of the model. The amount of voltage applied to the circuit can be changed, thereby changing the intensity of the gas discharge. The gas discharge current is closed when ionized working gas enters the area between the electrodes. A photo of the model in the nozzle with supersonic xenon flow is shown in Fig. 1, *c*.

The patterns of the flow around the model are visualized by the schlieren system (Fig. 1, *a*), where a pulsed semiconductor laser with a wavelength of 656 nm and a pulse duration of 30 ns is used as a point light source *5*. The source is located at a focal length from the input lens 6, which creates a parallel beam of light that illuminates a working area with a diameter of 100 mm in the area of the model location. The light is then focused by the output lens *8*, creating an image of the entrance slit in the area of the knife location *9*, as well as an image of the model on the recording matrix of the digital camera *10*. The knife blocks half of the illuminate light, which creates a background of illumination around the image of the model on the matrix of the Canon EOS 300D camera.

During the process of flow past the body, light from the source is refracted by density gradients, is cut off by the knife, or passes over it, making gas-dynamic discontinuities visible, including the BSW that forms during the supersonic flow around the test model. The main obstacle to obtaining high-quality images was the plasma's strong intrinsic glow. To reduce it, a filter was installed with a bandwidth in the wavelength range of 656 nm laser radiation, and a narrow collimator was placed in front of the knife. According to the flow patterns in different experiments, the distance d along the nozzle axis from the front surface of the body to the BSW was determined and the change in the position of the BSW depending on the organized flow conditions was studied.

It should be noted that the influence of the side walls on the flow and plasma effects was not taken into account, since preliminary studies showed that at the densities of the selected modes, the boundary layer build-up is weak, the sight glasses are made of optical glass, well polished, and the joints with the chamber walls were specially aligned. The electrodes mounted in the model do not come into contact with the side windows, and the gas-discharge current

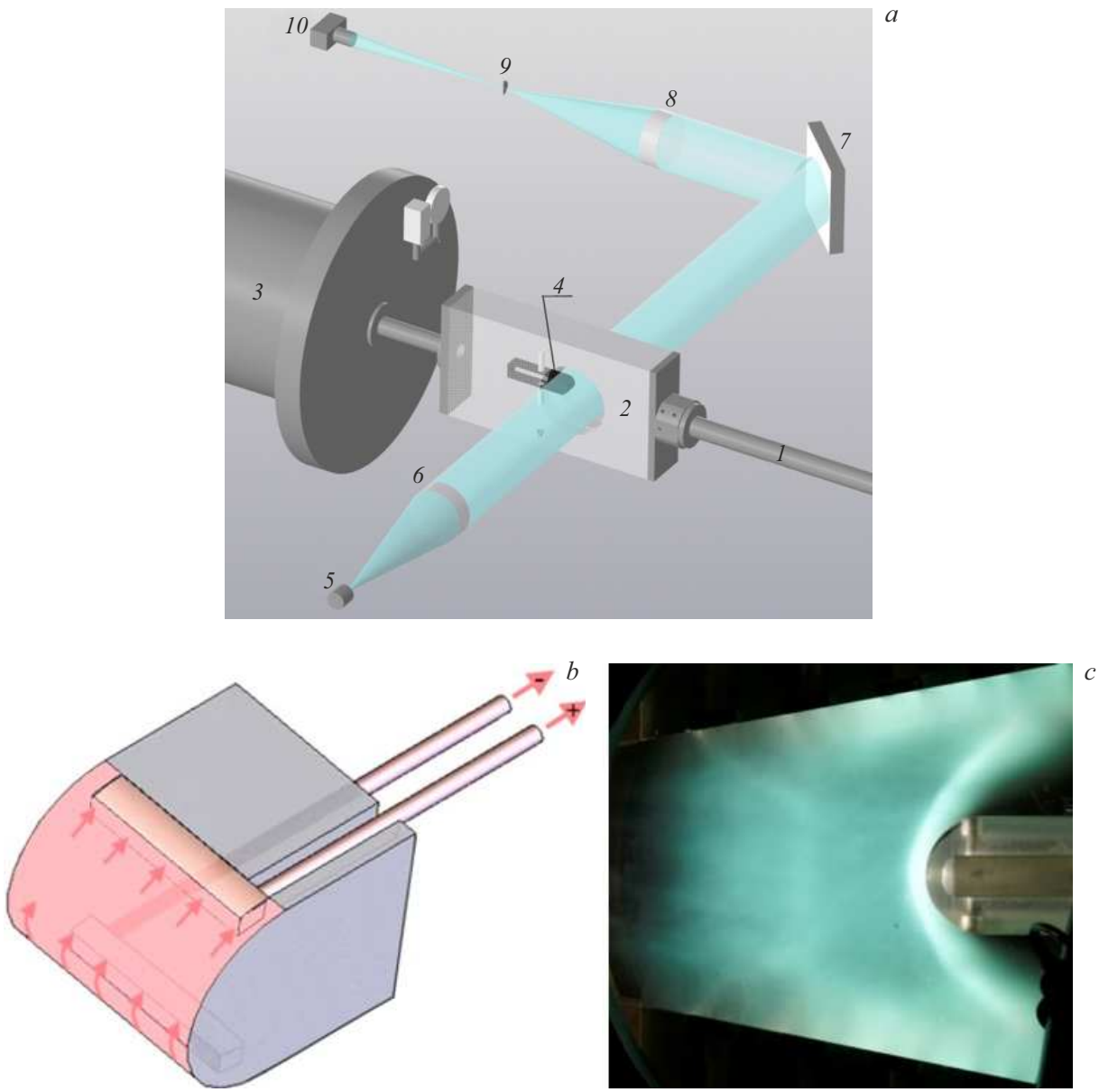

Figure 1. *a* — diagram of the experimental test bench; *b* — shape of the studied model; *c* — location of the model in the nozzle.

is shorted through the plasma medium in front of the body, which was checked by a glow from a side angle.

1.2. Selection of modes and parameters of the flow flowing onto the body

For studies with the working gas xenon, the shock tube operating mode was selected, characterized by the following parameters: pressure of the driver hydrogen gas $p_4 = 2.1 \cdot 10^6$ Pa, pressure in the low-pressure chamber $p_1 = 4000$ Pa and gas temperature $T_1 = 300$ K, the Mach number of the shock wave in the shock tube $M_2 = 8$. The mode allows obtaining a uniform flow of ionized xenon in the nozzle with a duration of up to 600 μs. The peculiarity of the gas discharges organized in operation is that the discharge is closed already in the presence of conductivity in the flow. The shock-compressed gas plug created in the shock tube is braked at the end of the tube, heats up due to the transfer of kinetic energy of the flow into heat, while creating an equilibrium xenon plasma with the following parameters: temperature of atoms $T_{5h} = 7700$ K and electrons $T_{5e} = 8700$ K, conductivity $\sigma_5 = 2500$ S/m, degree of ionization $\alpha_5 = 1.5 \cdot 10^{-2}$, concentration of atoms $n_{5h} = 0.9 \cdot 10^{25}$ m^{-3}. As the gas moves through the nozzle, it expands, and due to the relatively long relaxation time of xenon [18], the gas temperature decreases faster than the electron temperature. As a result, before the gas discharge is turned on, a stream of nonequilibrium plasma with the following parameters already runs to the body: Mach number of the flow $M = 6.8$, gas temperature

$T_h = 1200$ K, electron temperature $T_e = 3926$ K, conductivity $\sigma = 700$ S/m, degree of ionization $\alpha = 0.0018$, flow velocity $u = 2 \cdot 10^3$ m/s, gas density $\rho = 0.04$ kg/m^3, pressure $p = 3.1 \cdot 10^3$ Pa, concentration $n_h = 1.87 \cdot 10^{23}$ m^{-3} and $n_e = 3.37 \cdot 10^{20}$ m^{-3}.

The operating mode of the shock tube with the working gas air was chosen from the following considerations: the duration of the air flow sufficient for the formation of a stationary flow, the concentration of particles in the working part $n = 10^{23}-10^{24}$ m^{-3}, during expansion in the nozzle, the gas temperature T_h should remain above the condensation temperature of the air components and possible molecular impurities, the temperature of the air thermally heated behind the reflected shock wave at the end of the impact tube should not exceed the temperature at which a noticeable change in the molecular composition of the air occurs. In air, the relaxation of gas during expansion in the nozzle occurs very quickly, so weakly ionized gas flows to the body, the main ionization of the gas occurs during deceleration at the body and in the discharge. The experiment was carried out under the following operating conditions of the shock tube: initial pressure and temperature of the working gas $p_1 = 4000$ Pa, $T_1 = 300$ K, the Mach number of the shock wave in the shock tube $M_2 = 6.6$. Stagnation parameters before entering the nozzle: $p_5 = 1.91 \cdot 10^6$ Pa, $T_5 = 4710$ K. In the area of the body: $M = 4.15$, $T_h = 1300$ K, $u = 3 \cdot 10^3$ m/s, $\rho = 0.018$ kg/m^3, $p = 8 \cdot 10^3$ Pa.

Estimates of the adiabatic index in the flowing stream and in the area in front of the model were carried out in accordance with the theory [14], which assumes that in an ionized medium, the adiabatic index strongly depends on the degree of ionization and the degree of non-equilibrium of the medium, which can lead to both a decrease and an increase of it depending on ratios of plasma parameters. For the above parameters, in the flow incident on the model in xenon $\gamma = 1.217$, in air $\gamma = 1.323$. When decelerating near the leading edge of the model, the flow is additionally ionized, its parameters approach thermodynamically equilibrium, which leads to an increase in the adiabatic index in the region between the BSW and the frontal surface of the body. The initial value of γ in the exposure zone in the absence of a gas discharge in xenon was estimated as $\gamma_s = 1.258$, in the air due to weak ionization, the adiabatic index in the absence of a gas discharge was considered $\gamma_s = 1.323$.

1.3. Experimental discharge parameters at the leading edge of the model

A semi-cylindrical model with embedded electrodes was made to study the effect of a surface discharge on the position of the BSW. The electrodes are horizontally positioned on the surface of the cylindrical area of the body, as can be seen in Fig. 1, *b*. When a discharge is organized through these electrodes, the gas-discharge current covers the surface of the nasal part of the body along a semicircular trajectory. A specially designed LC circuit connected to the electrodes via a diagnostic resistance $R = 0.05\,\Omega$ is used as a voltage source, which makes it possible to organize a near-surface gas discharge of various gas discharge current strengths without additional keys, which is determined by the voltage applied to the circuit. Before the experiment, the LC circuit is charged to a preset voltage. The discharge is initiated by the arrival of an ionized stream into the area between the electrodes and covers the nasal part of the body along a semicircular trajectory. The discharge occupies an area of space near the body behind the shock wave with a size of approximately $L \times l \times h = 4.5 \times 5 \times 0.5$ cm. The impact begins at the moment of the beginning of the flow, and the formation of a steady BSW occurs already in the presence of a gas discharge zone. When braking at the surface of the body, the kinetic energy of the flow is converted into thermal energy, the gas is ionized behind BSW, its density and temperature increase, while the temperature state becomes close to equilibrium. A gas discharge increases both the degree of ionization in the region between the BSW and the model, and the temperature of the electrons and the gas as a whole, while changing the degree of non-equilibrium. These processes affect the adiabatic index of the medium, and consequently, the gas dynamic parameters of the flow.

The characteristic oscillograms of the gas-discharge current in the near-surface region and the plasma conductivity achieved in this case $\langle\sigma\rangle$ for experiments in xenon and in air are shown in Fig. 2. The current value in different experiments was changed by changing the value of the charging voltage of the LC circuit. The duration of the discharge was determined by the time when the model was streamlined by the plasma medium, i.e., by the size of the ionized gas plug. The duration of the plug of the shock-compressed gas in the impact tube in xenon and air differed by 3 times, as can be seen from the current waveforms.

The formation time of the stationary bow shock wave near the model is of the order 70 μs from the beginning

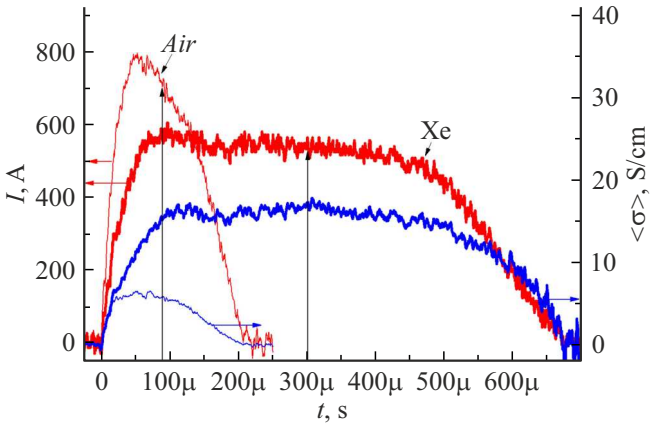

Figure 2. Oscillograms of discharge current (red curve) and conductivity (blue curve) of xenon and air plasma during surface discharge. Xenon — bold lines, air — thin lines.

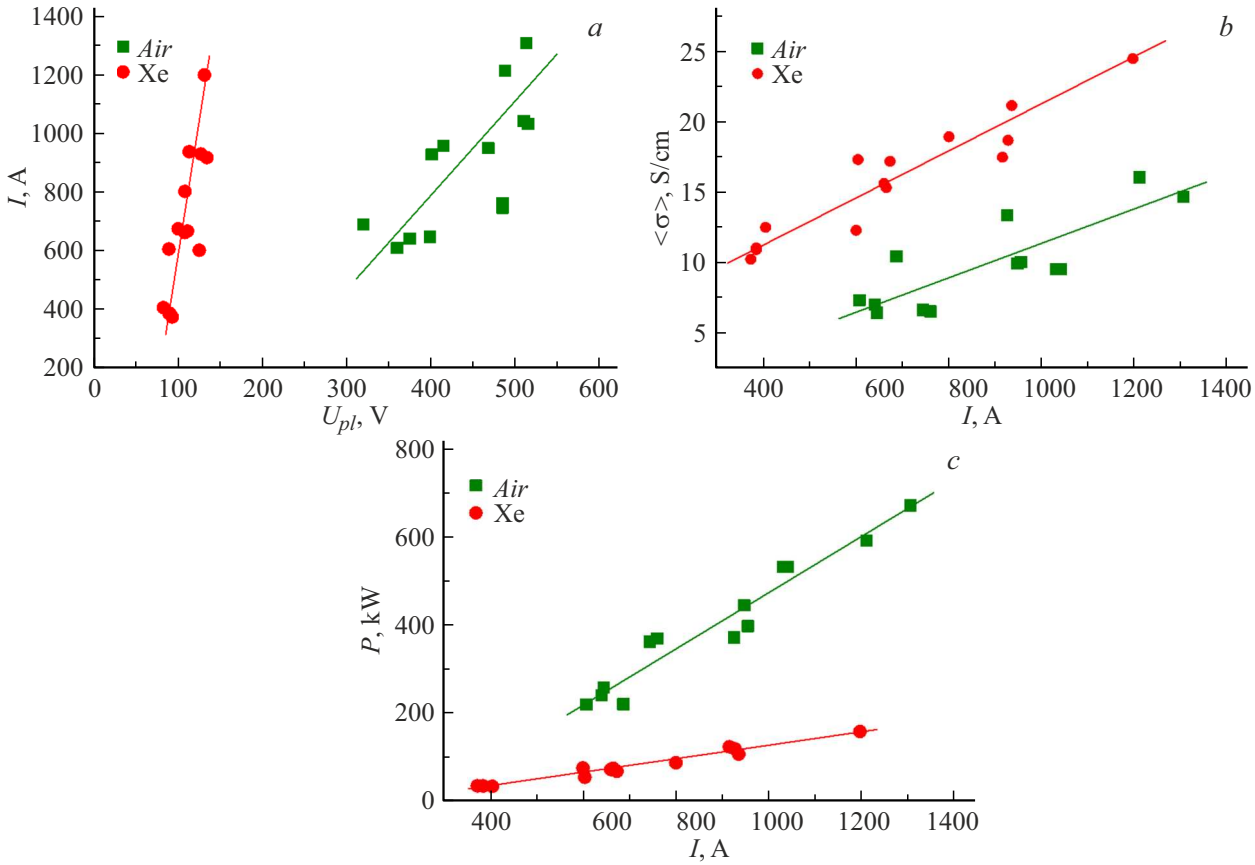

Figure 3. Volt-ampere characteristics (a), conductivity (b) and power (c) of a near-surface gas discharge in xenon (red circles) and air (green squares).

of the flow, followed by the stationary flow of the model. It is in this time area that the diagnosis of the flow takes place. The schlieren pattern is recorded in the region of stationary flow through 330 μs after the beginning of the flow in xenon and 90 μs in air. The moment of recording of schlieren patterns is shown by black vertical arrows in Fig. 2.

The parameters of the surface gas discharge acting on the flow were determined experimentally by the volt-ampere characteristics of the dependence of the gas-discharge current I on the voltage across the discharge gap U_{pl}, which is shown in Fig. 3, a. The resulting average effective air conductivity was determined according to the Ohm's law for plasma

$$j = \langle\sigma\rangle E,$$

where is the discharge current density

$$j = \frac{I}{S} = \frac{I}{hl},$$

and the electric field strength

$$E = \frac{U_{pl}}{L}.$$

The dependence of the average effective air conductivity obtained at the surface of the model in the discharge is shown in Fig. 3, b. It can be seen that in air, to achieve conductivities close to those of xenon, a much greater gas-discharge current must be organized. This means that in order to create a discharge intensity comparable to that in xenon, in an air discharge it is necessary to increase the electric field strength in the discharge gap and the power supplied to the discharge should be almost an order of magnitude greater than in xenon, as can be seen in Fig. 3, c.

1.4. Changing the flow pattern under surface plasma exposure

At different intensities of the gas surface discharge, schlieren patterns of flow around a semi-cylindrical body by a stream of xenon and an air stream were obtained. Examples of the obtained flow patterns of the model are shown in Fig. 4. The schlieren patterns were used to measure the relative stand-off of the BSW $(d-d_0)/d_0$, where d_0 is the distance between the BSW and the leading edge of the model during stationary flow in the absence of a discharge. Measurements for each position of the shock wave were carried out along the nozzle axis at different magnifications of the schlieren pattern, then the data were averaged. The uncertainty in finding the amount of stand-off is not more than 10 %. Experimental data have shown

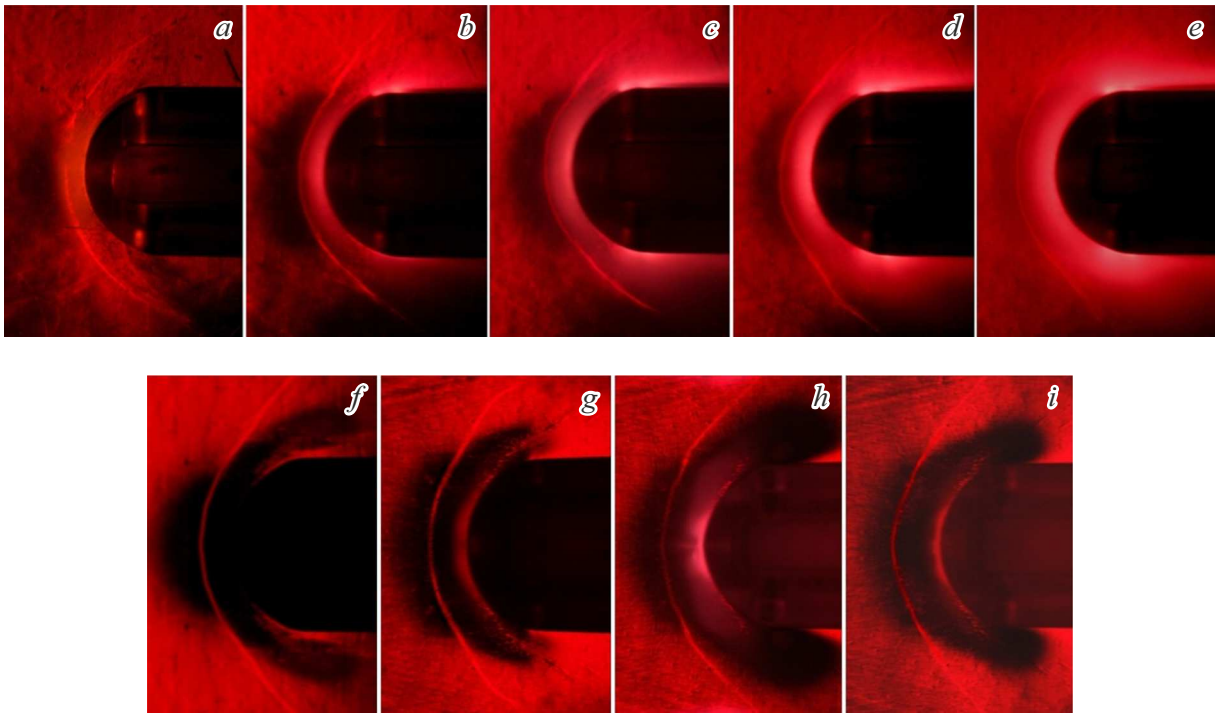

Figure 4. Schlieren flow patterns at different gas discharge intensities. Xenon: *a* — $I = 0$; *b* — $I = 370$ A, $P = 35$ kW; *c* — $I = 670$ A, $P = 66$ kW; *d* — $I = 915$ A, $P = 125$ kW; *e* — $I = 1200$ A, $P = 158$ kW. Air: *f* — $I = 0$; *g* — $I = 607$ A, $P = 220$ kW; *h* — $I = 760$ A, $P = 370$ kW; *i* — $I = 1040$ A, $P = 530$ kW.

that with an increase in the discharge intensity in the region between the BSW and the model, the stationary shock wave departs from the body, and the distance d increases both in xenon and in air. The stand-off of a stationary BSW under such an impact is determined by a combination of reasons. These are thermal effects, namely, gas heating due to heating in the discharge of charged particles and the transfer of thermal energy in collisions to neutral atoms and molecules, as well as plasma effects that affect the adiabatic index of the medium, on which the main parameters of the flow depend.

2. Numerical simulation

2.1. Methodology and problem statement

In the experiment, an ionized flow organized in a shock tube reaches the body and causes the ignition of a discharge between electrodes located on the body to which a voltage is applied. When the flow reaches the body, the formation of BSW begins, which passes through the zone of influence of the gas discharge plasma. In this case, additional ionization occurs in front of the body due to an increase in temperature behind the shock wave front. It should be noted that this additional ionization is present in a steady flow and in the absence of discharge impact. The calculations assume that the hot zone of ionized gas exposure in front of the body occurs instantly, due to the difference in the time scales of the development of discharge and gas dynamic phenomena. Thus, the effect of the discharge is modeled by the action of a volumetric gas region with increased energy and an altered adiabatic index. It should be noted that the calculations for xenon include the presence of additional ionization in front of the body, and in the calculations of air it is insignificant [16] and is not taken into account. In the figures below, the boundary of the discharge impact zone is indicated in red.

The simulation is based on the Navier–Stokes equations for a perfect viscous thermally conductive gas, the adiabatic index varied at different values of the specific discharge power q (power per unit mass). It was assumed that the flow is parallel to the axis of symmetry. The complete system of Navier–Stokes equations is solved numerically in divergent form for dimensionless variables [19]:

$$\frac{\partial \mathbf{U}}{\partial t} + \frac{\partial (\mathbf{F} + \mathbf{F}_v)}{\partial x} + \frac{\partial (\mathbf{G} + \mathbf{G}_v)}{\partial y} = \mathbf{H}, \tag{1}$$

$$\mathbf{U} = \begin{pmatrix} \rho \\ \rho u \\ \rho v \\ E \end{pmatrix}, \quad \mathbf{F} = \begin{pmatrix} \rho u \\ p + \rho u^2 \\ \rho uv \\ u(E + p) \end{pmatrix},$$

$$\mathbf{G} = \begin{pmatrix} \rho v \\ \rho uv \\ p + \rho v^2 \\ v(E + p) \end{pmatrix}, \quad \mathbf{H} = \begin{pmatrix} 0 \\ 0 \\ 0 \\ \rho q \end{pmatrix},$$

$$\mathbf{F}_v = -\begin{pmatrix} 0 \\ \frac{\mu}{\mathrm{Re}}(4/3u_x - 2/3v_y) \\ \frac{\mu}{\mathrm{Re}}(v_x + u_y) \\ \frac{\mu\pi_1}{\mathrm{Re}} + \frac{1}{\mathrm{N}}kT_x \end{pmatrix},$$

$$\mathbf{G}_v = -\begin{pmatrix} 0 \\ \frac{\mu}{\mathrm{Re}}(v_x + u_y) \\ \frac{\mu}{\mathrm{Re}}(4/3v_y - 2/3u_x) \\ \frac{\mu\pi_2}{\mathrm{Re}} + \frac{1}{\mathrm{N}}kT_y \end{pmatrix},$$

$$\pi_1 = u\big(4/3u_x - 2/3v_y\big) + v(v_x + u_y),$$

$$\pi_2 = v\big(4/3v_y - 2/3u_x\big) + u(v_x + u_y),$$

$$E = \rho\big(\varepsilon + 0.5(u^2 + v^2)\big), \quad N = \mathrm{Re}\,\mathrm{Pr}(\gamma - 1)/\gamma.$$

Here ρ, p, u, v is the gas density, pressure, x- and y-components of velocity. The specific power in the higher energy region of the gas formed by the discharge is q (where q is the variable parameter), and the specific internal energy of ε is

$$\varepsilon = p/\big(\rho(\gamma - 1)\big).$$

The Sutherland's law was used for the dependence of the dynamic viscosity μ on the temperature T for air

$$\mu = \frac{T^{1.5}(1 + s_1)}{T + s_1},$$

where $s_1 = 110\,\mathrm{K}$. For xenon, it was assumed that

$$\mu = T^{0.5}.$$

It was assumed that the coefficient of thermal conductivity k depends on temperature as

$$k = T^{0.5}.$$

The problem is solved in dimensionless variables, which are expressed in terms of dimensional variables (indicated by the index „dim“) as follows:

$$t = \frac{t_{dim}}{t_{n,}},\ x = \frac{x_{dim}}{l_{n,}},\ y = \frac{y_{dim}}{l_{n,}},\ u = \frac{u_{dim}}{u_{n,}},\ v = \frac{v_{dim}}{u_{n,}},$$

$$\rho = \frac{\rho_{dim}}{\rho_n},\ p = \frac{p_{dim}}{p_n},\ T = \frac{T_{dim}}{T_n}.$$

The following scaling factors were used in the calculations:

$$\rho_n = \rho_\infty, \quad p_n = p_\infty, \quad l_n = D, \quad T_n = T_\infty,$$

$$u_n = (p_\infty/\rho_\infty)^{0.5}, \quad t_n = l_n/u_n,$$

where the index ∞ defines the parameters of the oncoming flow. In the figures below, unless otherwise indicated, the values along the axes are shown in dimensionless form.

At the boundaries of the body, boundary conditions are used to ensure the absence of normal flows and the absence of slippage:

$$\frac{\partial p}{\partial n} = 0, \quad \frac{\partial T}{\partial n} = 0, \quad \mathbf{V} = 0.$$

No-reflection boundary conditions are used at the exit boundaries:

$$\frac{\partial p}{\partial n} = 0, \quad \frac{\partial T}{\partial n} = 0, \quad \frac{\partial \mathbf{V}}{\partial n} = 0,$$

where $\mathbf{V}$ is the flow velocity.

The initial conditions are the parameters of the oncoming flow: density ρ_∞, pressure p_∞ and velocity u_∞. For xenon, the problem was solved taking into account the initial increased ionization of the gas in front of the body.

The near-surface energy release is modeled by specifying a stationary region with a higher gas energy using the right-hand side of the energy equation in (1), where q is the specific power in this region. The width of this area in the direction x is selected by processing experimental schlieren patterns (Fig. 4). It is assumed that this region occurs instantly and is determined through the initial conditions and values of the specific power q and the adiabatic index of the gas-discharge plasma γ_s.

The simulation is performed using computational code based on complex conservative difference schemes [20], which have second-order accuracy in space and time. A five-point Lax scheme pattern is used to construct the scheme, resulting in staggered, orthogonal, and uniform grids throughout the computing domain. The differential consequences of the system (1) for partial derivatives with respect to x and with respect to y are used for the development of schemes to increase the order of approximation. Thus, in addition to the main conservative variables, their first derivatives with respect to x and y are used, which are considered as unknown functions and calculated using the same stencil. The necessary second derivatives are calculated using the values of the first derivatives at the nodes of the stencil.

In the chess grids used in calculations, the distance between the nodes is $2h_x$ and $2h_y$ (where h_x and h_y denote spatial steps along the directions x and y, respectively). The time step is selected using the Courant–Friedrichs–Levy criterion. Calculations were performed at $h_x = h_y = 0.001$ on the computation domains containing about $6 \cdot 10^6$ nodes (counting the middle node of the template).

The boundaries of an aerodynamic body are introduced into the computational domain without violating conservation laws in it. The curved boundary fits into a rectangular staggered difference grid by constructing difference schemes in the vicinity of the boundary using new types of stencils based on 1/4, 1/2 and 3/4 parts of the cell. Such incomplete cells are adjacent to complete standard cells, ensuring compliance with conservation laws in the entire computational domain, including areas adjacent to the boundaries of the body. The details of constructing difference schemes in the computational domain and in the vicinity of the boundaries of the aerodynamic body, as well as a number of test variants are presented in Ref. [20]. The analysis of grid convergence is given in Ref. [16,17].

Table 1. Determining the parameters of the incoming flow and normalization coefficients for modeling the effects of a near-surface discharge in xenon and in air

	Description	Dimensional value	Dimensionless value	Normalizing coefficient
Xenon	Mach number of the incoming flow, M_∞		6.8	
	Adiabatic index in the incoming flow, γ		1.217	
	Reynolds number, Re		4558.9	
	Prandtl number, Pr		0.623	
	Pressure in the incoming flow, p_∞	$3.1 \cdot 10^3$ Pa	1.0	$p_n = p_\infty$
	Density in the incoming flow, ρ_∞	0.040793 kg/m^3	1.0	$\rho_n = \rho_\infty$
	Temperature in the oncoming flow T_∞	1200 K	1.0	$T_n = T_\infty$
	Specific power in the plasma region q		0, 52, 82.5, 119.5, 147.2, 213.3	$q_n = p_n/(t_n\rho_n) = 0.698299 \cdot 10^6$ kW/kg
	Speed, u	2067.96 m/s	7.502	$u_n = (p_n/\rho_n)^{0.5} = 275.668$ m/s
	Time, t		1.0	$t_n = l_n/u_n = 108.827\,\mu$s
Air	Mach number of the incoming flow, M_∞		4.153	
	Adiabatic index in the incoming flow, γ		1.323	
	Reynolds number, Re		6763.2	
	Prandtl number, Pr		0.703	
	Pressure in the oncoming flow, p_∞	6790.546 Pa	1.0	$p_n = p_\infty$
	Density in the incoming flow, ρ_∞	0.017572 kg/m^3	1.0	$\rho_n = \rho_\infty$
	Temperature in the oncoming flow, T_∞	1302.024 K	1.0	$T_n = T_\infty$
	Specific power in the plasma region, q		0, 43, 55, 57, 75, 130	$q_n = p_n/(t_n\rho_n) = 8.00763 \cdot 10^6$ kW/kg
	Speed, u	2969.272 m/s	4.776	$u_n = (p_n/\rho_n)^{0.5} = 621.64$ m/s
	Time, t		1.0	$t_n = l_n/u_n = 48.26\,\mu$s

2.2. Numerical results on bow shock wave control in xenon and air

The determining flow parameters and normalization coefficients used in modeling the effects of near-surface discharge in xenon and in air are given in Table 1.

Fig. 5 illustrates the steady-state flow regime under the influence of the energy of a near-surface discharge on the position of the BSW at time $t = 2.0$. Stationary density fields in isochores for different values of specific power are shown (images are superimposed). It can be seen that the higher the value of the specific power q, the farther the BSW is from the body in the stationary mode.

The mechanism of influence on the position of the stationary BSW of the near-surface energy storage is set in Ref. [16] and is related to the fact that the BSW during its formation moves through an already existing heated region of gas discharge plasma (due to the difference in the time scales of the formation of the discharge plasma zone and gas dynamic processes). Thus, the parameters of the discharge zone have an effect on the parameters of the forming BSW at the non-stationary stage of the flow, and therefore, these parameters determine the position of the BSW at the stationary stage.

Fig. 6 illustrates the dynamics of x-coordinate of the BSW front when the values of q change during the establishment of a steady flow. The position of the BSW was determined by selecting the coordinate x, corresponding to the maximum value of p_x at the wave front. It should be noted that the presence of fluctuations in these dependences is due to the discreteness of the representation of the shock wave front in the difference cell associated with the construction of an algorithm for tracking the BSW front. Fig. 6 for air shows tangents to curves that have different angles of inclination to the axis x. This means that the speed of the BSW at the non-stationary stage is also different for different values of q, and this speed is higher for large q. Thus, when BSW passing through the discharge plasma region, the higher the specific power value, the further the BSW is removed from the body,

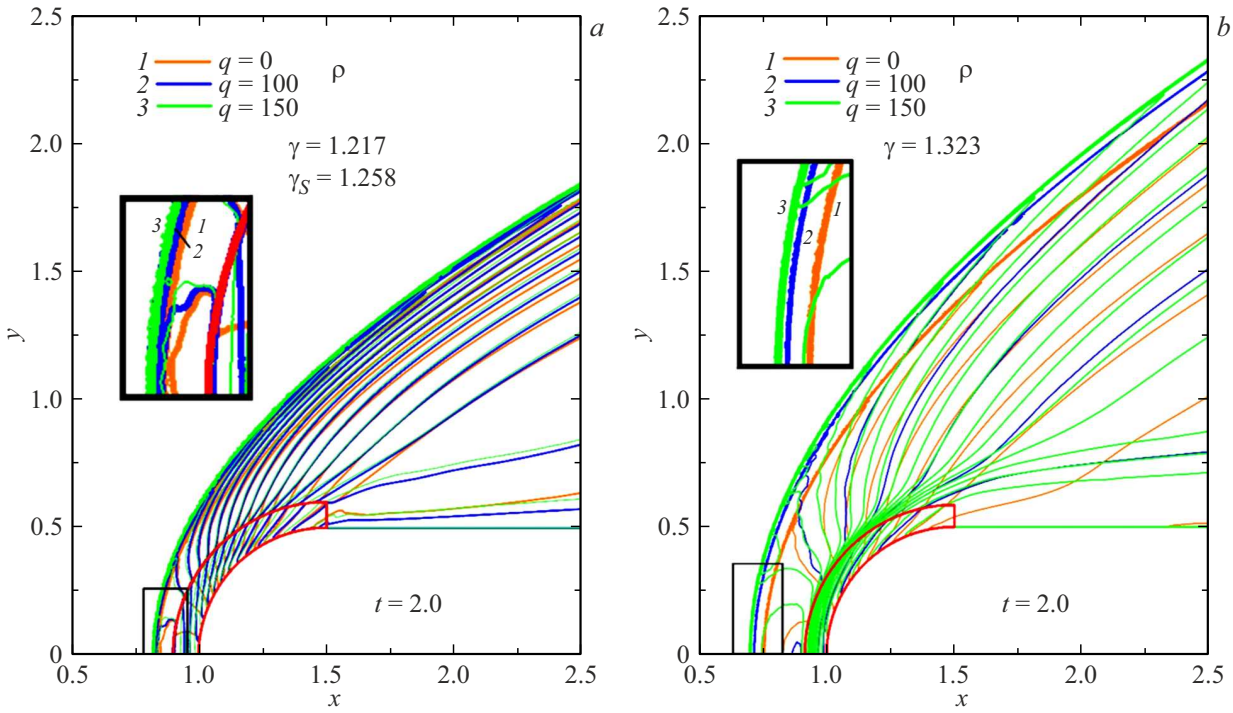

Figure 5. Density fields in isochores for different specific power values q, $t = 2.0$: a — xenon, $M = 6.8$, $\gamma = 1.217$, $\gamma_s = 1.258$; b — air, $M = 4.15$, $\gamma = 1.323$, $\gamma_s = 1.323$.

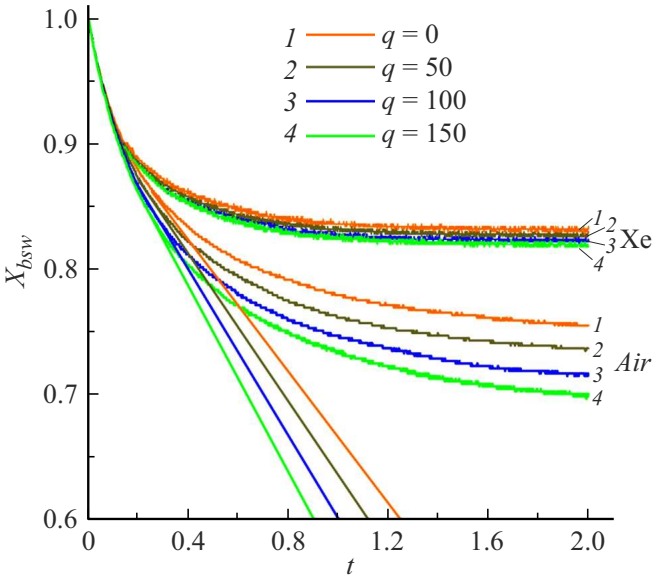

Figure 6. Dynamics of x-coordinate of the BSW at various values q in the process of establishing a steady-state flow regime in xenon and in air.

which affects the position of the BSW in the stationary flow mode. It should be noted that since the distance to the BSW directly affects the aerodynamic characteristics of a streamlined body, the ability to influence the position of the BSW means the ability to control the aerodynamics of a flying object.

The effect of the near-surface plasma region on the aerodynamic characteristics of a streamlined body was studied in Ref. [16] in air and in Ref. [17] in xenon at the Mach numbers of the incident flow 4.1 and 6.8, respectively. The dynamics of density, pressure, temperature, and relative drag forceF/F_0 when their values are set at the braking point on the cylinder for various values of the specific power of the plasma region q. Here the drag force is

$$F = \int_0^{0.5D} p_b \, dy,$$

where p_b is pressure on the cylindrical part of the body surface, F_0 is the drag force F without energy input.

The results given in Ref. [16,17] indicate the fact that at the stagnation point at the steady stage, the pressure shows only slight changes with increasing q, while the rarefaction of the gas increases markedly, which leads to a significant increase in temperature. In the same place, it was found that the relative drag force F/F_0 acting on the frontal surface of the body decreases with increasing BSW distance from the body. In the stationary mode, this force is slightly greater for higher q values, as shown in the provided figures in Ref. [16,17].

Calculations have shown that significant changes in temperature and density occur in the near-surface area due to the release of discharge energy. It is also established that the position of the BSW in the steady state depends on the adiabatic index of the gas discharge plasma γ_s. The density fields for stationary flow regimes at $q = 100$ and varying

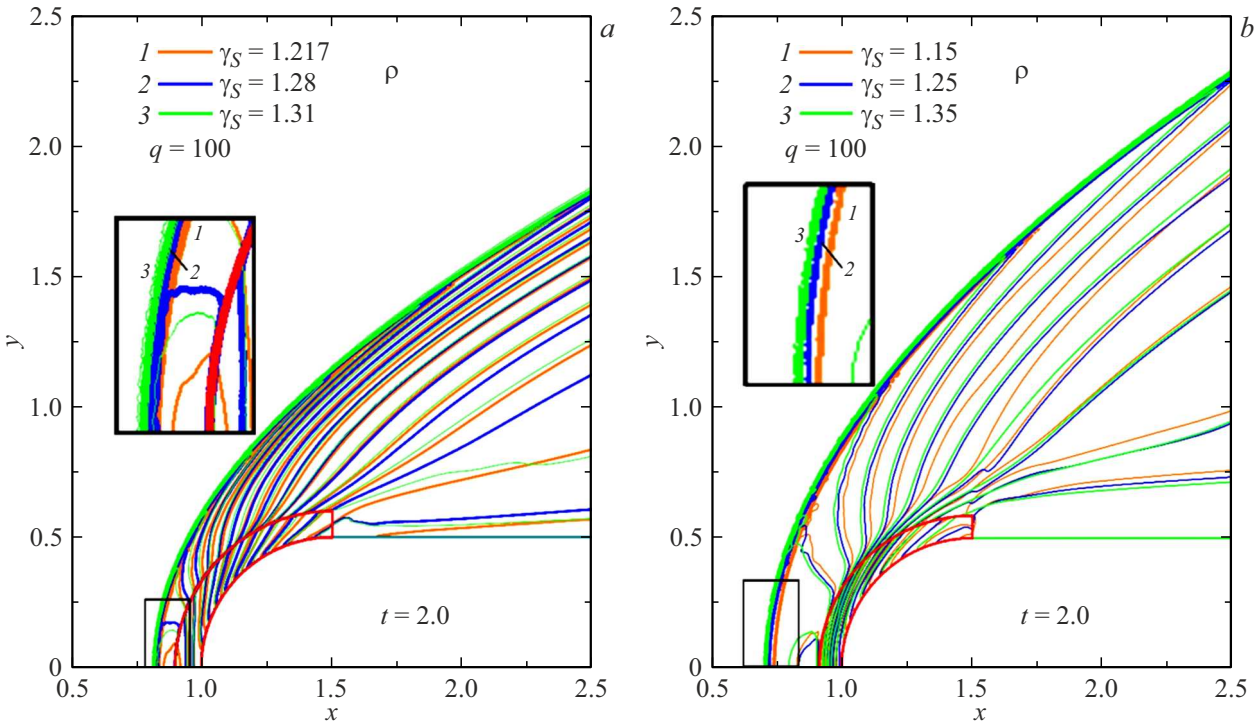

Figure 7. Density fields in isochores for various plasma adiabatic index values γ_s, $q = 100$, $t = 2.0$: *a* — xenon, $M = 6.8$, $\gamma = 1.217$; *b* — air, $M = 4.15$, $\gamma = 1.323$.

values of γ_s, shown in Fig. 7, illustrate the fact that a greater value of γ_s corresponds to a greater stand-off of the steady BSW. It has been found that in flows with Mach numbers up to 7 , the position of the stationary BSW reacts even to a slight change of γ_s, and the lower the Mach number of the flow, the easier it is to control the position of the steady BSW by changing γ_s. It should be noted that a constant value of the specific discharge power means constant Joule heating provided by the discharge, and the dynamics of γ_s is determined by the degree of ionization and the degree of disequilibrium in the plasma zone [14]. Thus, Fig. 7 reflects the influence of purely plasma parameters on the steady position of the BSW.

2.3. Comparison of experimental and numerical results

The calculated and experimental dependences of the relative stand-off of the steady BSW from the aerodynamic body as a function of the discharge power for xenon and air are shown in Fig. 8. Here, when modeling the xenon flow, additional plasma ionization was taken into account for the BSW in the plasma region in front of the model (initial value of $\gamma_s = 1.258$ [17]). It is obvious from Fig. 8 that the steady-state relative values of the stand-off are determined by two parameters q and γ_s, and with increasing current and discharge power, the adiabatic index tends to increase in xenon and decrease in air. It is also found that the relative stand-off values obtained experimentally

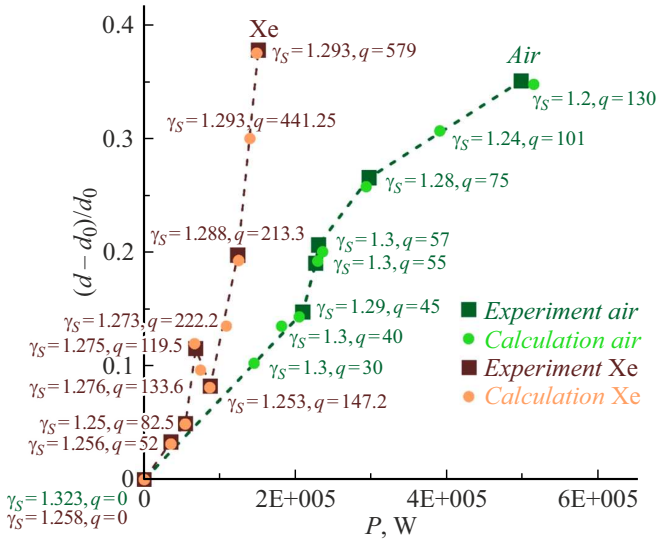

Figure 8. Dependence of the relative magnitude of the stationary BSW from the discharge power in xenon and air.

and in the simulation are consistent. The dependence of relative stand-off on discharge power is close to linear at the initial stage (in xenon for $0 < P < 54.2$ kW, in air for $0 < P < 240$ kW). In addition, an oscillation of relative stand-off was obtained in xenon at $54.2 < P < 86.6$ kW. This fluctuation can be explained by the fact that the adiabatic index γ_s strongly depends on the degree of

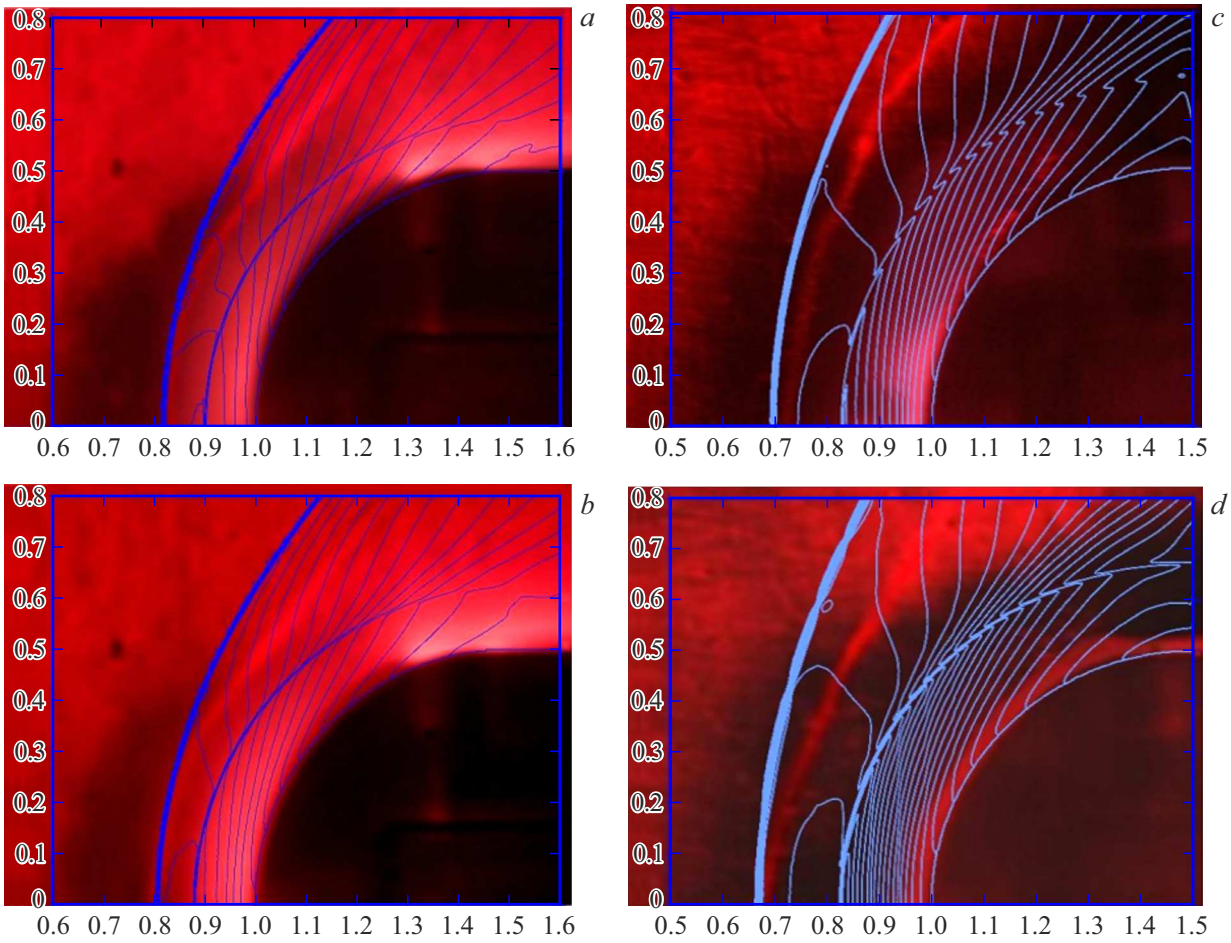

Figure 9. Comparison of numerical flow patterns with schlieren images under the influence of a near-surface discharge in xenon (left) and in air (right): *a* — $I = 670$ A, $P = 66$ kW, $\gamma_s = 1.275$, $q = 119.5$; *b* — $I = 915$ A, $P = 125$ kW, $\gamma_s = 1.288$, $q = 213.3$; *c* — $I = 760$ A, $P = 370$ kW, $\gamma_s = 1.28$, $q = 75$; *d* — $I = 1040$ A, $P = 530$ kW, $\gamma_s = 1.2$, $q = 130$.

Table 2. Correspondence between the discharge current I, the specific power q and the adiabatic index of the gas-discharge plasma γ_s in xenon and air

Xenon	I, A	0	373	604	673	800	915	1196
	q	0	52	82.5	119.5	147.2	213.3	579
	$q_{dim} \cdot 10^{-6}$ kW/kg	0	36.312	57.610	83.447	102.790	148.947	404.315
	γ_s	1.258	1.256	1.25	1.275	1.253	1.288	1.293
Air	I, A	0	607	640	645	760	900	1040
	q	0	45	55	57	75	101	130
	$q_{dim} \cdot 10^{-6}$ kW/kg	0	360.34	440.42	456.43	600.57	705.28	1041.0
	γ_s	1.323	1.29	1.3	1.3	1.28	1.24	1.2

ionization in this range of discharge currents, which can lead to both its increase and decrease [17].

Fig. 9 shows a comparison of numerical flow patterns and schlieren flow images under the influence of a near-surface discharge in xenon and air. The discrepancy between the calculated and experimental shape of the shock wave at the periphery is due to the divergent flow structure in the nozzle. Some discrepancy between the calculated and experimental images in Fig. 9, *c* is explained by the fact that the initial conditions for air do not take into account the additional ionization of the body flow (this discrepancy is absent when considering relative stand-off).

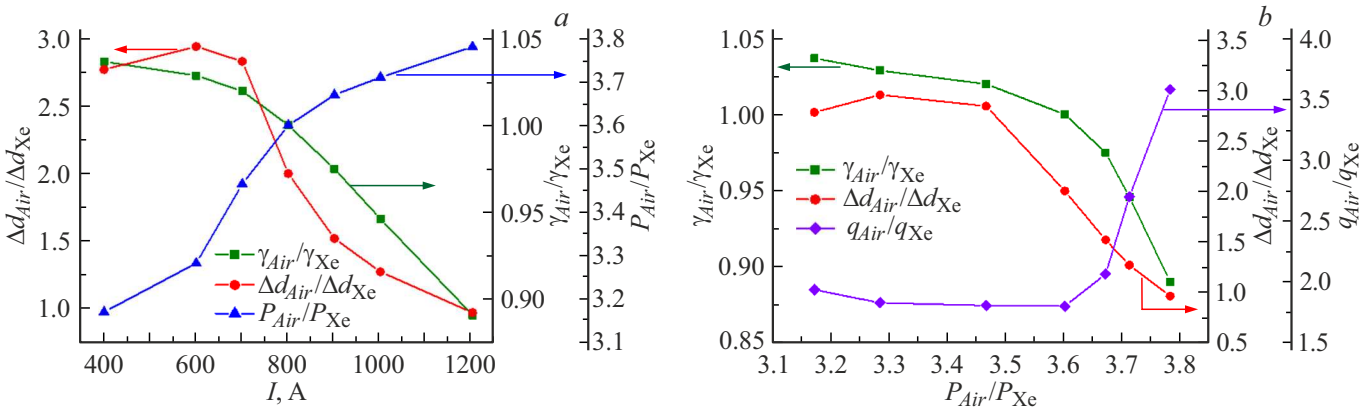

Figure 10. The ratio of relative stand-off (red circles), discharge capacities (blue triangles) and adiabatic indices (green squares), and specific capacities (purple diamonds) in the air to the corresponding parameters in xenon, depending on: *a* — the magnitude of the gas discharge current; *b* — the ratio of the powers of the discharges.

It can be noted that the numerical and experimental flow patterns correspond to the position of the BSW on the axis of symmetry for the obtained parameters γ_s and q, the estimated size of the discharge plasma region, and the established initial conditions for the incident flow in the case of xenon and air.

Table 2 shows the correspondence between the specific power generated by the discharge q, the discharge current I and the value of the adiabatic index in the discharge zone γ_s for xenon and air. Here q_{dim} is the dimensional value of the specific power q. It can be seen that in xenon, with increasing discharge current, the specific power increases; the adiabatic index γ_s remains almost unchanged in the range 1.25−1.258 (up to the value of the discharge current $I = 604$ A), then there is an oscillation γ_s to a value of 1.275. At higher values of the discharge current, the adiabatic index γ_s increases to 1.293. In air, as the discharge current increases, the specific power also increases; the adiabatic index γ_s remains almost unchanged in the range 1.3−1.323 (up to the value of the discharge current $I = 645$ A). At higher values of the discharge current, the adiabatic index γ_s decreases.

3. Discussion of results

A generalized analysis of the experimental and numerical modeling data for xenon and air was carried out. The value of the gas-discharge current at the surface of the model was chosen as a comparison criterion. For this purpose, the dependences of the main parameters on the gas discharge current were constructed and the ratios of the corresponding parameters in air to the value of this parameter in xenon were taken. Fig. 10, *a* shows the dependences of the ratios of the relative stand-off of the steady BSW $\Delta d = (d - d_0)/d_0$, discharge capacities and adiabatic parameters of the gas discharge plasma on the discharge current. It can be seen that at low current values of up to 600 A the rate of increase of the stand-off of the BSW is greater in the air than in xenon, but as the current increases, the rate of increase of stand-off in xenon becomes greater and significantly exceeds the rate of increase of BSW stand-off in air. At $I = 1200$ A, the relative stand-off value in different gases is the same, but at the same time, to achieve the same stand-off, the discharge power in air must be almost 4 times greater than in xenon. The increase in gas-discharge current is accompanied by a decrease in the ratio of stand-off distances of the stationary BSW and an increase in the power ratio. The ratio of the air adiabatic index to the xenon adiabatic index decreases both with increasing current and with increasing power ratio (Fig. 10, *b*). It can be noted that the adiabatic parameters in gas-discharge plasma in diatomic and monatomic gases are close in value and become the same at a current of 800 A and the ratio of discharge powers 3.6. Up to these values of current and power, the ratio of specific powers practically does not change, with a further increase in current and discharge power, a sharp increase in the ratio of specific powers is observed, which indicates a significant superiority of the power required for further impact on the position of the BSW, invested in a unit mass of air plasma compared with xenon at high discharge intensities.

Conclusion

The paper presents experimental and numerical results of a study of the effect of a near-surface plasma region near an aerodynamic body formed during the organization of a gas discharge in xenon and air on the position of a stationary bow shock wave. Fields of flow parameters are obtained for different values of the specific discharge power q and the adiabatic index γ_s in the plasma region created by the gas discharge. A comparison of the numerical and experimental values of the relative stand-off of the steady bow shock wave demonstrated their good agreement. The following new results were obtained:

— it was demonstrated the possibility to control the BSW and aerodynamic characteristics of a body in gases with different adiabatic indices due to the formation of a volumetric plasma region, which is formed using a surface gas discharge organized on the entire frontal surface of the body;

— it was established that the position of the stationary BSW is determined by the specific discharge power and the value of the adiabatic index (which is influenced by the degree of ionization and the degree of non-equilibrium) in the plasma zone created by the discharge. At the same time, the adiabatic index of the gas-discharge plasma plays a significant role in the dynamics of the flow structure and in the magnitude of the stand-off of the stationary BSW from the body;

— it was found that at the initial stage (in xenon for $0 < P < 54.2\,\text{kW}$, in air for $0 < P < 240\,\text{kW}$) the dependence of relative stand-off on discharge power is close to linear, at the same time, the adiabatic index is close to constant ($1.258 < \gamma_s < 1.253$ in xenon, $1.3 < \gamma_s < 1.323$ in air). In xenon, an uneven stand-off of the BSW from the body in the steady flow stage was obtained at the discharge power $54.2 < P < 86.6\,\text{kW}$;

— it was found that for active control of the position of the BSW in the air, the power of the surface gas discharge must be almost 4 times greater than the power in xenon; with increasing current, the ratio of discharge power in air to power in xenon increases, while the ratio of relative stand-off and the adiabatic index decrease. It was found that the adiabatic values in air and xenon in gas-discharge plasma are close in value and become the same at a discharge current of 800 A and the power input into xenon of 95 kW and into air of 345 kW. From the same values of current and power, there is a strong increase in the specific power in the air discharge compared with the discharge in xenon.

Thus, the possibility of controlling both the stationary position of the BSW and the characteristics of an aerodynamic body in gases with different adiabatic indices by creating a volumetric plasma region in front of its entire frontal surface by varying the plasma adiabatic index and the energy characteristics of the discharge has been demonstrated. The results obtained have the potential to develop control systems for high-speed flows, taking into account not only thermal effects, but also the influence of plasma parameters.

Funding

This study was supported by the Ministry of Science and Higher Education of the Russian Federation, project №075-15-2024-544.

Conflict of interest

The authors declare that they have no conflict of interest.

References

[1] D. Knight. J. Propulsion Power, **24**, 1153 (2008). DOI: 10.2514/1.24595
[2] M.Y.M. Ahmed, N. Qin. Progress Aerospace Sci., **112**, 100585 (2020). DOI: 10.1016/j.paerosci.2019.100585
[3] S. Rashid, F. Nawaz, A. Maqsood, S. Salamat, R. Riaz. Proc. Institution of Mechanical Engineers, Part G: J. Aerospace Engineering, **12**, 2851 (2022). DOI: 10.1177/09544100211069796
[4] O.A. Azarova, O.V. Kravchenko. Energies, **17** (7), 1632 (2024). DOI: 10.3390/en17071632
[5] S.B. Leonov, I.V. Adamovich, V.R. Soloviev. Plasma Sources Sci. Technol., **25**, 063001 (2016). DOI: 10.1088/0963-0252/25/6/063001
[6] P. Yu. Georgievskij, V.A. Levin. Pis'ma v ZhTF, **14** (8), 684 (1988) (in Russian).
[7] V.I. Artemyev, V.I. Bergelson, I.V. Nemchinov et al. Izvestiya AN SSSR. MZhG, **5**, 146 (1989) (in Russian).
[8] P.K. Tretyakov, V.M. Fomin, V.I. Yakovlev. *Proc. Int. Conf. Methods of Aerophysical Research* (Novosibirsk, Russia, 1996), p. 210.
[9] V.A. Bityurin, A.I. Klimov, S.B. Leonov, et al. In: *Proc. 3rd Weakly Ionized Gases Workshop* (Norfolk, AIAA, 1999), p. 4940. DOI: 10.2514/6.1999-4940
[10] V.P. Fomichev, M.A. Yadrenkin. Pisma v ZhTF, **43** (23), 31 (2017) (in Russian). DOI: 10.21883/PJTF.2017.23.45273.16648
[11] H. Yan, F. Liu, J. Xu, Y. Xue. AIAA J., **56**, 532 (2017). DOI: 10.2514/1.J056107
[12] B. Tang, S. Guo, L. Hua. Contributions to Plasma Phys., **61** (2), e202000067 (2020). DOI: 10.1002/ctpp.202000067
[13] O.A. Azarova, A.V. Erofeev, T.A. Lapushkina. Pisma v ZhTF, **43** (8), 93 (2017). (in Russian) DOI: 10.21883/PJTF.2017.08.44540.16598
[14] K.T.A.L. Burm, W.J. Goedheer, D.C. Schram. Phys. Plasmas, **6**, 2622 (1999). DOI: 10.1063/1.873535
[15] V. Lago, R. Joussot, J. Parisse. J. Physics D: Appl. Phys., **47**, 125202 (2014). DOI: 10.1088/0022-3727/47/12/125202
[16] O.A. Azarova, T.A. Lapushkina, Y.A. Shustrov. Phys. Fluids, **34**, 066117 (2022). DOI: 10.1063/5.0093787
[17] O.A. Azarova, T.A. Lapushkina, O.V. Kravchenko. Fluids, **9** (12), 277 (2024). DOI: 10.3390/fluids9120277
[18] Yu.P. Raiser. *Fizika gazovogo razryada* (Nauka, M., 1987) (in Russian).
[19] P. Rouch. *Vychislitel'naya gidrodinamika* (Mir, M., 1980) (in Russian).
[20] O.A. Azarova. ZhVM i MF, **55** (12), 2067 (2015) (in Russian). DOI: 10.7868/S0044466915120030

Translated by A.Akhtyamov